

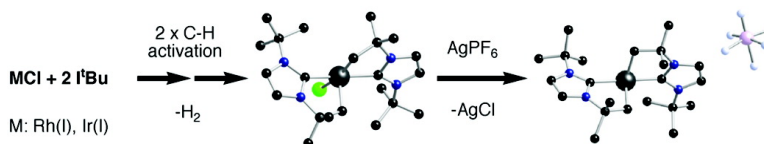
Article

Interaction of a Bulky *N*-Heterocyclic Carbene Ligand with Rh(I) and Ir(I). Double C–H Activation and Isolation of Bare 14-Electron Rh(III) and Ir(III) Complexes

Natalie M. Scott, Reto Dorta, Edwin D. Stevens, Andrea Correa, Luigi Cavallo, and Steven P. Nolan

J. Am. Chem. Soc., **2005**, 127 (10), 3516-3526 • DOI: 10.1021/ja043249f • Publication Date (Web): 19 February 2005

Downloaded from <http://pubs.acs.org> on March 24, 2009



More About This Article

Additional resources and features associated with this article are available within the HTML version:

- Supporting Information
- Links to the 34 articles that cite this article, as of the time of this article download
- Access to high resolution figures
- Links to articles and content related to this article
- Copyright permission to reproduce figures and/or text from this article

[View the Full Text HTML](#)

Interaction of a Bulky *N*-Heterocyclic Carbene Ligand with Rh(I) and Ir(I). Double C–H Activation and Isolation of Bare 14-Electron Rh(III) and Ir(III) Complexes

Natalie M. Scott,[†] Reto Dorta,[†] Edwin D. Stevens,[†] Andrea Correa,[‡]
Luigi Cavallo,[‡] and Steven P. Nolan^{*,†}

Contribution from the Department of Chemistry, University of New Orleans,
New Orleans, Louisiana 70148, and Dipartimento di Chimica, Università di Salerno,
Baronissi (SA) 84081, Italy

Received November 9, 2004; E-mail: snolan@uno.edu

Abstract: Reactivity and structural studies of unusual rhodium and iridium systems bearing two *N*-heterocyclic carbene (NHC) ligands are presented. These systems are capable of intramolecular C–H bond activation and lead to coordinatively unsaturated 16-electron complexes. The resulting complexes can be further unsaturated by simple halide abstraction, leading to 14-electron species bearing an all-carbon environment. Saturation of the vacant sites in the 16- and 14-electron complexes with carbon monoxide permits a structural comparison. DFT calculations show that these electrophilic metal centers are stabilized by π -donation of the NHC ligands.

Introduction

The wide interest in the synthesis of coordinatively unsaturated metal complexes arises from their central role as intermediates in many stoichiometric and catalytic processes.¹ In the context of catalytic C–H bond activation and functionalization, d⁶ 14-electron metal complexes are of special importance. Such four-coordinate, 14-electron d⁶-ML₄ complexes are generally transient species that are formed in situ by ligand dissociation. Due to the exceptionally high Lewis acidity inherent in these 14-electron metal complexes, they tend to interact with even the weakest of nucleophiles and the empty coordination sites are most commonly filled by counterions,² or by weakly coordinating solvent molecules such as alcohols, THF, acetone, or methylene chloride.^{3,4} Recent efforts, notably by Caulton et al., have shown that, by using bulky phosphine ligands and non-coordinating anions, fully characterized 14-electron d⁶-ML₄ compounds can indeed be synthesized. Examples of crystallographically characterized compounds are very rare and are

limited to two Ir(III) and three Ru(II) compounds.^{4a,5,6} Fourteen-electron Rh(III) compounds have so far eluded isolation.⁷ Crucial to the stability of these highly unsaturated metal centers is the additional σ -donation offered through agostic interactions with C–H bonds of the bulky phosphine ligands surrounding the metal center.^{8,9} These and analogous results on 14-electron d⁸-ML₃ compounds have led to the concept that bare 14-electron complexes will not be stable or isolable as such.¹⁰

The current research effort in the area of *N*-heterocyclic carbene (NHC) complexes of late transition metals originated from the desire to develop highly active, phosphine-free catalysts.¹¹ While the use of NHCs has proven advantageous in a number of catalytic processes, these ligand systems are only starting to emerge as possible candidates for stabilizing unusual metal complexes.¹² Recent theoretical and experimental

[†] University of New Orleans.

[‡] Università di Salerno.

- (1) Collman, J. P.; Hegedus, L. S.; Norton, J. R.; Finke, R. G. In *Principles and Applications of Organotransition Metal Chemistry*; University Science: Mill Valley, CA, 1987.
- (2) For a very recent example, see: (a) Rifat, A.; Kociok-Köhn, G.; Steed, J. W.; Weller, A. S. *Organometallics* **2004**, *23*, 428–432. For a review, see: (b) Strauss, S. H. *Chem. Rev.* **1993**, *93*, 927–942.
- (3) An important series of LTM complexes stabilized by O-bound ligands comprises the catalytically active [M(H)₂(PR₃)₂(S)]⁺ (M = Rh, Ir; S = alcohol, THF, H₂O, acetone) species. Two such compounds have been characterized crystallographically; see: (a) Crabtree, R. H.; Hlatky, G. G.; Parnell, C. P.; Segmüller, B. E.; Uriarte, R. J. *Inorg. Chem.* **1984**, *23*, 354–358. (b) Luo, X.-L.; Schulte, G. K.; Crabtree, R. H. *Inorg. Chem.* **1990**, *29*, 682–686.
- (4) For η^2 -coordination of CH₂Cl₂ to a 14-electron Ru(II) complex, see: (a) Huang, D.; Huffman, J. C.; Streib, W. E.; Bollinger, J. C.; Eisenstein, O.; Caulton, K. G. *J. Am. Chem. Soc.* **1997**, *119*, 7398–7399. For a review on halocarbon coordination to unsaturated d⁶ complexes, see: (b) Kulawiec, R. J.; Crabtree, R. H. *Coord. Chem. Rev.* **1990**, *99*, 89–115.

- (5) (a) Cooper, A. C.; Streib, W. E.; Eisenstein, O.; Caulton, K. G. *J. Am. Chem. Soc.* **1997**, *119*, 9069–9070. (b) Cooper, A. C.; Clot, E.; Huffman, J. C.; Streib, W. E.; Maseras, F.; Eisenstein, O.; Caulton, K. G. *J. Am. Chem. Soc.* **1999**, *121*, 97–106.
- (6) (a) Baratta, W.; Herdtweck, E.; Rigo, P. *Angew. Chem., Int. Ed.* **1999**, *38*, 1629–1631. (b) Watson, L. A.; Ozerov, O. V.; Pink, M.; Caulton, K. G. *J. Am. Chem. Soc.* **2003**, *125*, 8426–8427.
- (7) Recent publications by Werner et al. and Milstein et al. show that while neutral compounds of this type are dimeric, cationic complexes are stabilized by counterions or solvent molecules: (a) Canepa, G.; Brandt, C. D.; Werner, H. J. *Am. Chem. Soc.* **2002**, *124*, 9666–9667. (b) Gandelman, M.; Konstantinovskii, L.; Rozenberg, H.; Milstein, D. *Chem. Eur. J.* **2003**, *9*, 2595–2602.
- (8) For reviews on agostic interactions, see: (a) Brookhart, M.; Green, M. L. H.; Wong, L. *Prog. Inorg. Chem.* **1988**, *36*, 1–124. (b) Crabtree, R. H. *Angew. Chem., Int. Ed. Engl.* **1993**, *32*, 789–805.
- (9) σ -Donation through agostic interactions might be comparable in strength to σ -donation by acetone; see: Dorta, R.; Goikhman, R.; Milstein, D. *Organometallics* **2003**, *22*, 2806–2809.
- (10) (a) Strauss, S. H. *Chemtracts: Inorg. Chem.* **1994**, *6*, 1–13. (b) Casares, J. A.; Espinet, P.; Salas, G. *Chem. Eur. J.* **2002**, *8*, 4843–4853.
- (11) (a) Herrmann, W. A. *Angew. Chem., Int. Ed.* **2002**, *41*, 1290–1309. (b) Bourissou, D.; Guerret, O.; Gabbai, F. P.; Bertrand, G. *Chem. Rev.* **2000**, *100*, 39–91. (c) Arduengo, A. J., III; Harlow, R. L.; Kline, M. *J. Am. Chem. Soc.* **1991**, *113*, 361–363.

work in our group has shown that NHC ligands are more electron-donating than even basic alkylphosphines. More importantly, both IAd and I^tBu ligands (IAd = *N,N*-di(adamantyl)imidazol-2-ylidene, I^tBu = *N,N*-di(*tert*-butyl)imidazol-2-ylidene) appear to be substantially more bulky than sterically demanding phosphine ligands such as P^tBu₃.¹³ We reasoned that reactivity studies involving the very bulky and basic I^tBu with appropriate Rh(I) and Ir(I) precursors might allow for the isolation of stable, unsaturated, and high-valent compounds via intramolecular C–H activation.¹⁴

Here, we report on the interaction of I^tBu with [M(CO)₂Cl]₂ (M = Rh, Ir), which results in a unique double cyclometalation process of the NHC ligand system at room temperature and ultimately leads to the synthesis and structural characterization of unprecedented examples of bare, 14-electron d⁶-RhL₄ and d⁶-IrL₄ metal complexes. DFT calculations on these complexes provide an explanation for their stability and uncover a surprising electronic aspect of the *N*-heterocyclic carbene ligand class. Furthermore, reactivity studies show that while these complexes do not coordinate ligands such as THF, acetone, or dichloromethane, they react cleanly with carbon monoxide to give rare examples of all-carbon bound d₆-ML₆ compounds. Some experimental data on the Rh system described here have been published as a communication.¹⁵

Results and Discussion

Interaction of I^tBu with [Rh(CO)₂Cl]₂. To avoid any unwanted reactivity between the solvent and the metal precursors and/or the NHC ligands, reactivity studies between I^tBu and [M(CO)₂Cl]₂ were carried out in hydrocarbon solvents only. As a starting point, we investigated the reactivity of a hexane slurry containing [Rh(CO)₂Cl]₂ with a slight excess of I^tBu (4.16 equiv). Stirring this slurry at room temperature for 4 h afforded an almost limpid yellow solution. Concentration and subsequent addition of pentane led to the precipitation of RhClH(I^tBu)(I^tBu') (**2**; Scheme 1) as a yellow solid in high yield. X-ray-quality crystals of **2** were obtained by slow evaporation of a saturated hexane solution. Its structure is represented in Figure 1, and selected bond distances and angles can be found in Table 1. As anticipated, one of the NHC ligands is cyclometalated (I^tBu'), with the metalated CH₂ group *cis* to the hydride ligand and *trans* to the chloride and the second I^tBu. Most significantly, the empty coordination site in this 16-electron complex is taken up by a rather strong agostic interaction from one of the ^tBu groups of the non-metalated I^tBu ligand. The agostic interaction of the *tert*-butyl groups with the rhodium metal center shows distances of 2.073 Å [Rh(1)–H(16A)] and 2.704 Å [Rh(1)–C(16)], with a second hydrogen

Scheme 1. Reactivity of I^tBu with [M(CO)₂Cl]₂

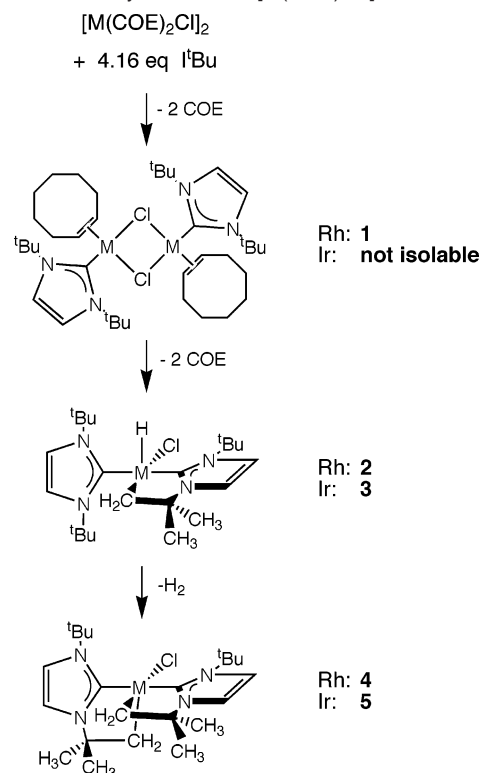


Table 1. Selected Bond Lengths (Å) and Angles (deg) for RhClH(I^tBu)(I^tBu') (**2**) and IrClH(I^tBu)(I^tBu') (**3**)

complex 2		complex 3	
Rh1–C1	2.081	Ir1–C1	2.029
Rh1–C12	2.058	Ir1–C12	2.048
Rh1–C5	2.074	Ir1–C5	2.112
Rh1–Cl	2.530	Ir1–Cl	2.513
Rh1–H1	1.430	Ir1–H1	1.390
Rh1···C16	2.704	Ir1···C16	2.700
Rh1···H16A	2.073	Ir1···H16A	2.018
Rh1···H16B	2.653	Ir1···H16B	2.669
C1–Rh1–C12	169.499	C1–Ir1–C12	169.961
C1–Rh1–C5	79.002	C1–Ir1–C5	79.210
C1–Rh1–Cl	104.927	C1–Ir1–Cl	104.075
C1–Rh1–H1	88.723	C1–Ir1–H1	86.793

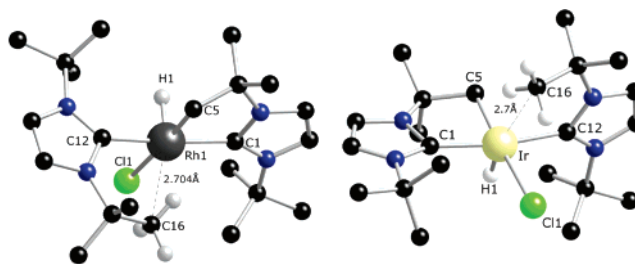


Figure 1. Ball-and-stick representations of complexes RhClH(I^tBu)(I^tBu') (**2**; left) and IrClH(I^tBu)(I^tBu') (**3**; right).³¹

atom at 2.653 Å [Rh(1)–H(16B)].¹⁶ The nature of the agostic interaction in **2** was studied by variable-temperature ¹H NMR spectroscopy in toluene-*d*₈. Data recorded at room temperature show that all signals for the cyclometalated I^tBu' ligand give rise to sharp resonances. Interestingly, both the hydride peak

- (12) (a) Jazzar, R. F. R.; Macgregor, S. A.; Mahon, M. F.; Richards, S. P.; Whittlesey, M. K. *J. Am. Chem. Soc.* **2002**, *124*, 4944–4945. (b) Clement, N. D.; Cavell, K. J.; Jones, C.; Elsevier, C. *J. Angew. Chem., Int. Ed.* **2004**, *43*, 1277–1279. (c) Caddick, S.; Cloke, F. G. N.; Hitchcock, P. B.; Lewis, A. K. *Angew. Chem., Int. Ed.* **2004**, *43*, 5824–5827.
- (13) (a) Hillier, A. C.; Sommer, W. J.; Yong, B. S.; Peterson, J. L.; Cavallo, L.; Nolan, S. P. *Organometallics* **2003**, *22*, 4322–4326. (b) Dorta, R.; Stevens, E. D.; Hoff, C. D.; Nolan, S. P. *J. Am. Chem. Soc.* **2003**, *125*, 10490–10491. (c) Dorta, R.; Stevens, E. D.; Scott, N. M.; Costabile, C.; Cavallo, L.; Hoff, C. D.; Nolan, S. P. *J. Am. Chem. Soc.* **2005**, *127*, 2485–2495.
- (14) Whereas such cyclometalation processes are well-documented and rather common for bulky phosphine and nitrogen-donor ligands, they have been rarely observed in NHCs. An example of intramolecular C–H activation of an NHC on Rh (using the less bulky and less basic IMes ligand) has appeared: Huang, J.; Stevens, E. D.; Nolan, S. P. *Organometallics* **2000**, *19*, 1194–1197.
- (15) Dorta, R.; Stevens, E. D.; Nolan, S. P. *J. Am. Chem. Soc.* **2004**, *126*, 5054–5055.

- (16) A discussion on nonclassical vs classical agostic interactions can be found in the following reference: Baratta, W.; Mealli, C.; Hertweck, E.; Inco, A.; Mason, S. A.; Rigo, P. *J. Am. Chem. Soc.* **2004**, *126*, 5549–5562.

(at -22.93 ppm) and the resonances associated with the agostic t -Bu ligand are broad, indicating a fluxional exchange of the t -butyl groups.¹⁷ The existence of this agostic bond in solution seems also to be reflected in the chemical shift value of the hydride ligand *trans* to it. In fact, signals of hydrides *trans* to an empty site for Rh(III) compounds are normally found at significantly higher field than the value here.^{18,19} When the temperature is gradually lowered, a sharpening of the peaks associated with t -Bu is observed. At 243 K, the spectrum of the agostically bound ligand shows two separate signals for the imidazole backbone protons, indicating a different influence of the two t -Bu groups (agostic and non-agostic, respectively) on the imidazole ring. The protons of the agostic and pendant t -Bu groups display two separate singlet resonances in the aliphatic region, each integrating for nine protons. All three CH_3 groups of the agostic t -Bu remain equivalent on the ^1H NMR time scale, implying a very small rotational barrier for these methyl groups. To establish whether coalescence of pendant and agostic t -Bu groups was observable, the sample was heated to 323 K. At this temperature, the pale yellow color of **2** slowly changes to orange. More importantly, formation of a new set of resonances is observed alongside extensive H/D scrambling between the deuterated solvent and complex **2**.

This latter result indicated that a different outcome might be observed when the reaction between t -Bu and $[\text{Rh}(\text{COE})_2\text{Cl}]_2$ is carried out in benzene. Indeed, stirring a benzene solution of $[\text{Rh}(\text{COE})_2\text{Cl}]_2$ with a slight excess of t -Bu (4.16 equiv) at room temperature for 4 h and subsequent workup of the reaction mixture gave a dark yellow solid in 88% yield. The ^1H NMR data are consistent with formation of the unusual, doubly cyclometalated complex $\text{RhCl}(\text{I}^t\text{Bu})_2$ (**4**). The proton spectrum features two doublets at 6.61 and 6.42 ppm for the imidazole backbone protons. The cyclometalated CH_2 groups give rise to two separate signals, a doublet at 2.21 ppm and a doublet of doublets at 2.92 ppm. This additional doublet signal is due to $J_{\text{Rh-H}}$ coupling of one proton of each CH_2 group with the metal center, while the other doublets arise from geminal coupling ($J_{\text{H-H}} = 10$ Hz). The ^{13}C NMR supports these data and shows one resonance at low field for the carbenic carbons ($J_{\text{Rh-C}} = 43.1$ Hz) and one signal at 28.97 ppm for the CH_2 groups ($J_{\text{Rh-C}} = 34.7$ Hz). To ascertain the exact structure of complex **4**, X-ray-quality crystals were grown from a hexane solution. The unsaturated complex **4** displays a distorted square pyramidal structure around the rhodium center (Figure 2, bond lengths and angles in Table 2). Analogous to **2**, the two carbenic carbon atoms are disposed *trans* to each other at an angle of 167.43° with their corresponding cyclometalated CH_2 groups mutually *cis* (90.58°). One of the t -Bu groups of the ligand approaches the empty coordination site, but the distances to the metal center indicate no efficient agostic interaction in this case [2.557 Å for $\text{Rh}(1)\text{-H}(9\text{C})$ and 3.165 Å for $[\text{Rh}(1)\text{-C}(9)]$].²⁰

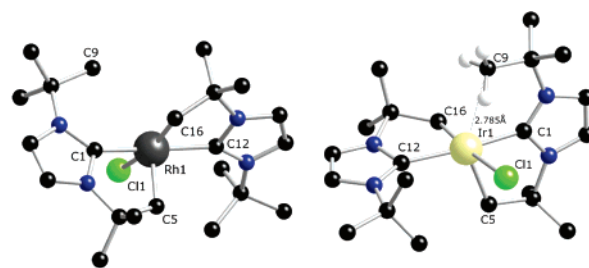


Figure 2. Ball-and-stick representations of complexes $\text{RhCl}(\text{I}^t\text{Bu})_2$ (**4**; left) and $\text{IrCl}(\text{I}^t\text{Bu})_2$ (**5**; right).

Table 2. Relevant Bond Lengths (Å) and Angles (deg) for $\text{RhCl}(\text{I}^t\text{Bu})_2$ (**4**), $\text{IrCl}(\text{I}^t\text{Bu})_2$ (**5**), $\text{RhCl}(\text{I}^t\text{Bu})_2(\text{CO})$ (**8**), and $\text{IrCl}(\text{I}^t\text{Bu})_2(\text{CO})$ (**9**)

	4	5	8	9
M1–C1	2.008(1)	1.981(16)	2.085(11)	2.075(8)
M1–C5	2.032(1)	2.210(20)	2.123(12)	2.128(9)
M1–C12	2.111(2)	2.103(16)	2.087(11)	2.075(8)
M1–C16	2.044(1)	2.081(15)	2.076(11)	2.090(8)
M1–C11	2.521(2)	2.509(4)	2.551(3)	2.513(3)
M1–C23			1.950(13)	2.013(10)
C1–M1–C5	81.06(6)	76.8(7)	80.4(5)	80.1(3)
C1–M1–C16	88.71(6)	90.9(6)	88.9(5)	88.7(3)
C1–M1–C12	167.43(5)	171.0(6)	163.7(4)	162.5(3)
C1–M1–C11	91.03(4)	83.6(4)	83.8(3)	84.3(2)
C16–M1–C11	167.10(4)	174.3(4)	172.7(3)	172.6(2)
C12–M1–C11	101.40(4)	105.4(4)	106.5(3)	106.0(2)
C23–M1–C1			105.3(5)	105.4(3)
C23–M1–C5			173.6(5)	174.4(3)
C23–M1–C12			88.1(5)	88.7(3)

To establish whether complex **4** is obtained through initial formation of **2**, we monitored the reaction between $[\text{Rh}(\text{COE})_2\text{Cl}]_2$ and t -Bu (4.16 equiv) by ^1H NMR in C_6D_6 . Indeed, during the first hour, the formation of **2** as indicated by a strong signal for the hydride at -23 ppm is observed. This was followed, after ca. 1 h, by the appearance of a characteristic peak at 4.74 ppm (solubilized H_2) and concomitant formation of the resonances for **4**.²¹ In addition, the doubly cyclometalated complex **4** is also obtained from a benzene solution containing isolated **2**.²²

The solvent-dependent reactivity of $[\text{Rh}(\text{COE})_2\text{Cl}]_2$ with t -Bu described above seems to stem from different solubilities of complexes **2** and **4** and from different polarities associated with the solvents used. This prompted us to investigate the reaction between $[\text{Rh}(\text{COE})_2\text{Cl}]_2$ and t -Bu (4.16 equiv) in pentane. To our delight, we were able to isolate the mixed dimer $[\text{Rh}(\text{COE})(\text{I}^t\text{Bu})\text{Cl}]_2$ (**1**) selectively by appropriately choosing the reaction conditions. When a dilute pentane slurry of $[\text{Rh}(\text{COE})_2\text{Cl}]_2$ (1 mL/4 mg) is treated with t -Bu (4.16 equiv), initial dissolution is observed (10 min), and after 30 min, a heavy pale-yellow precipitate containing **1** is formed.²³ Decanting the supernatant solution and washing the solid with pentane gives pure **1** in high yield. Instead, if the pentane suspension containing **1** is treated in situ with additional benzene and stirred overnight,

(17) Similarly fluxional behavior has recently been observed in a Ru–NHC complex; see: Abdur-Rashid, K.; Fedorkiw, T.; Lough, A. J.; Morris, R. H. *Organometallics* **2004**, *23*, 86–94.

(18) (a) Masters, C.; Shaw, B. L. *J. Chem. Soc. A* **1971**, 3680–3686. (b) Moulton, C. J.; Shaw, B. L. *J. Chem. Soc., Dalton Trans.* **1976**, 1020–1024. (c) Empsall, H. D.; Hyde, E. M.; Mentzer, E.; Shaw, B. L. *J. Chem. Soc., Dalton Trans.* **1977**, 2285–2291.

(19) The value found in **2** is similar to values for hydrides *trans* to O-bound ligands; see: (a) Schrock, R. R.; Osborn, J. A. *J. Am. Chem. Soc.* **1976**, *98*, 8, 2134–2142. (b) Rybtchinski, B.; Konstantinovskiy, L.; Shimon, L. J. W.; Vignalok, A.; Milstein, D. *Chem. Eur. J.* **2000**, *6*, 3287–3292.

(20) These distances might indicate a very weak agostic interaction; for comparison, see: Neve, F.; Ghedini, M.; Crispini, A. *Organometallics* **1992**, *11*, 3324–3327.

(21) Complex **2** can be isolated on a preparative scale by decreasing the reaction time in benzene to 1 h, but contamination by already formed **4** is usually observed.

(22) Reaction times are longer than for the in situ reaction and allowed characterization by ^{13}C NMR of **2** in benzene.

(23) Dilution is important for the outcome of this reaction. When the reaction is carried out in a more concentrated pentane slurry/solution, the yellow precipitate contains various amounts of **2** (up to 30%).

dissolution of **1** and formation of **4** are observed. On the other hand, isolated **1** (without the presence of excess ^tBu) is stable in a benzene solution. These control experiments convincingly demonstrate that complex **1** represents a precursor on the way to **2** and **4**. Furthermore, they show that the presence of only one electron-donating ^tBu ligand is not sufficient to favor intramolecular C–H activation and that the first cyclometalation process probably proceeds through initial formation of Rh-(^tBu)₂Cl. Complex **1** was fully characterized by NMR spectroscopy and elemental analysis. The proton spectrum shows resonances at 6.53 and 2.17 ppm (both singlets) for the ^tBu ligand and a broad signal at 2.61 ppm for the olefinic protons of COE. The ¹³C NMR gives doublets for the carbenic (at 178.30 ppm) and the olefinic (at 58.51 ppm) carbon atoms. Crystals of **1** were subjected to an X-ray analysis, and although the data set was somewhat poor and precluded a detailed discussion of its solid-state structure, the connectivity of **1** could be established and confirmed its dimeric nature.

Interaction of ^tBu with [Ir(COE)₂Cl]₂. The reactivity described above prompted us to investigate the interaction between the analogous iridium precursor and ^tBu. Reaction of [Ir(COE)₂Cl]₂ with 4.16 equiv of ^tBu in benzene affords the metalated hydride complex IrClH(^tBu)(^tBu') (**3**) after 20 h at room temperature (Scheme 1). Complex **3** was isolated as a yellow-green solid in nearly quantitative yield. Proton NMR (C₆D₆) data at room temperature essentially replicate the spectrum of the rhodium complex at low temperatures and indicate the presence of a somewhat stronger agostic interaction in **3**. The cyclometalated ^tBu arm shows two distinct doublet signals for the CH₂ group and two resonances for the C(CH₃)₂-CH₂ protons. The protons of the two imidazole rings give rise to four separate signals at 6.78, 6.69, 6.49, and 6.41 ppm, indicating a different influence of the two ^tBu groups on the imidazole ring of the non-metalated ^tBu ligand. More importantly, three different resonances are detected for the three non-cyclometalated ^tBu groups, again reflecting the chemical inequivalence of the two ^tBu groups of the non-metalated ^tBu ligand. The presence of the agostic interaction in **3** and its ability to alter the electronic properties via σ-donation from its C–H bond are especially apparent when looking at the hydride signal. Whereas signals of hydrides *trans* to an empty site in Ir(III) complexes are found at –43 ppm or lower,²⁴ the spectrum of **3** gives a singlet resonance for the hydride ligand at –32.83 ppm. This chemical shift value clearly suggests that the hydride is *trans* to another ligand (i.e., the agostic interaction) and parallels the electronic situation found for iridium(III) hydrides that are *trans* to O-bound ligands such as THF, acetone, or alcohols.²⁵

Well-formed single crystals were grown by direct reaction of [Ir(COE)₂Cl]₂ with 4.16 equiv of ^tBu in a more concentrated benzene solution that was kept under constant shaking (!). A representation of complex **3** is displayed in Figure 1, and important bond lengths and angles can be found in Table 1.

The structure is entirely consistent with the solution spectrum of this compound and closely resembles complex **2**. Again, one of the ^tBu groups of the non-metalated ^tBu ligand is involved in an agostic interaction from the C–H bond to the unsaturated iridium center. This strong agostic interaction is characterized by an Ir···C(16) distance of 2.700 Å, with one of the located and refined protons pointing toward the metal center [Ir···H(16C) = 2.018 Å] and a second proton [H(16B)] at 2.669 Å.

Complex **3** undergoes a second cyclometalation involving the agostically bonded ^tBu ligand. In fact, when a benzene solution containing **3** is stirred at room temperature for 4 days, workup yields the doubly cyclometalated complex IrCl(^tBu)₂ (**5**) in quantitative yield as a dark red solid (Scheme 1). It is worth noting that the same complex can also be synthesized in high yield directly from [Ir(COE)₂Cl]₂ and 4.16 equiv of ^tBu (C₆H₆, room temperature, 5 days). X-ray-quality crystals of complex **5** were obtained by slow evaporation of a dichloromethane solution, and its structure is shown in Figure 2. Bond lengths and angles are given in Table 2. The 16-electron complex **5** displays a distorted square pyramidal structure around the iridium center, and its overall structure is similar to the rhodium analogue **4**. One clear difference is that, in the solid-state structure of **5**, the sixth coordination site is taken up by an agostic interaction, showing bond distances of 2.785 Å [Ir(1)–C(9)] and of 2.039 Å [Ir(1)–H(9C)] to the metal center. Contrary to both hydride complexes **2** and **3**, the ¹H NMR spectrum of **5** does not give any indication for the agostic ^tBu group and displays only one resonance for both ^tBu groups (1.72 ppm).²⁶

The reaction between [Ir(COE)₂Cl]₂ and ^tBu (4.16 equiv) in hexanes and pentane was also investigated. Unfortunately, several attempts to synthesize the mixed dimer [Ir(COE)(^tBu)Cl]₂ were unsuccessful. To gain a better understanding of the differences between the Rh and Ir systems, we prepared C₆D₆ solutions of [M(COE)₂Cl]₂ with only 2 equiv of ^tBu (i.e., L:M = 1:1) and monitored the progress of these reactions by NMR spectroscopy. In the Ir case, the only products that could be detected were **3** and unreacted [Ir(COE)₂Cl]₂. The same reaction with Rh, while substantially more rapid (as seen by the faster disappearance of the signals for free ^tBu), gave a mixture of [Rh(COE)₂Cl]₂, **1**, and **2** → **4**. These results indicate that the relative rates for the individual steps leading to the cyclometalated product MClH(^tBu)(^tBu') are different for Rh and Ir, and that displacement of the first COE by ^tBu in [Ir(COE)₂Cl]₂ is far slower than the subsequent reactions, precluding isolation of the mixed dimer [Ir(COE)(^tBu)Cl]₂.

The reactivity displayed here between ^tBu and Rh(I)/Ir(I) is highly unusual. For instance, double cyclometalations of other ligand systems such as bulky phosphines or nitrogen-based systems have very rarely been observed for iridium,²⁷ and are unknown altogether for rhodium. To the best of our knowledge, this is also the first time that activation of a C–H bond by Rh(III) is directly observed.²⁸ It is also worth noting that, while agostic interactions between C–H bonds and metal centers are

(24) See ref 9 and the following references: (a) Masters, C. J.; Shaw, B. L.; Stainbank, R. E. *J. Chem. Soc., Chem. Commun.* **1971**, 209. (b) Moulton, C. J.; Shaw, B. L. *J. Chem. Soc., Dalton Trans.* **1976**, 1020–1024. (c) Kanzelberger, M.; Singh, B.; Czerw, M.; Krogh-Jespersen, K.; Goldman, A. S. *J. Am. Chem. Soc.* **2000**, *122*, 11017–11018. (d) Ben-Ari, E.; Gandelman, M.; Rozenberg, H.; Shimon, L. J. W.; Milstein, D. *J. Am. Chem. Soc.* **2003**, *125*, 4716–4717.

(25) (a) Crabtree, R. H.; Mellea, M. F.; Mihelcic, J. M.; Quirk, J. M. *J. Am. Chem. Soc.* **1982**, *104*, 107–113. (b) Crabtree, R. H.; Demou, P. C.; Eden, D.; Mihelcic, J. M.; Parnell, C. A.; Quirk, J. M.; Morris, G. E. *J. Am. Chem. Soc.* **1982**, *104*, 6994–7001.

(26) VT NMR studies (tol-*d*₈) show that the spectrum of **5** remains virtually unchanged in the range 297–233 K.

(27) We are aware of one such example, involving double cyclometalation on an Ir-PCP system; see: Mohammad, H. A. Y.; Grimm, J. C.; Eichele, K.; Mack, H.-G.; Speiser, B.; Novak, F.; Quintanilla, M. G.; Kaska, W. C.; Mayer, H. A. *Organometallics* **2002**, *21*, 5775–5784

(28) Activation of aryl C–H bonds by Rh(III) has been proposed in the catalytic transfer dehydrocoupling of arenes and silanes: Ezbiansky, K.; Djurovich, P. I.; LaForest, M.; Sinning, D. J.; Zayes, R.; Berry, D. H. *Organometallics* **1998**, *17*, 1455–1457 and references therein.

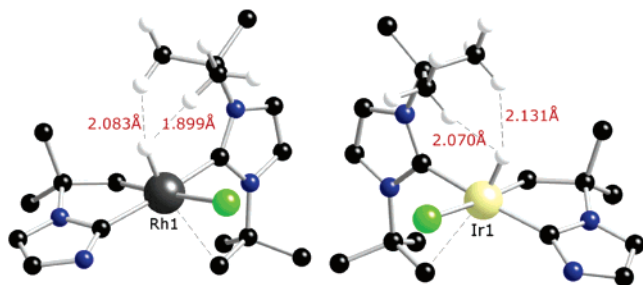
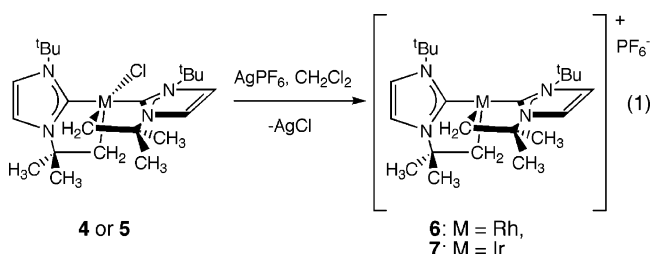


Figure 3. Partial views of $\text{RhClH}(\text{I}'\text{Bu})(\text{I}'\text{Bu}')$ (**2**; left) and $\text{IrClH}(\text{I}'\text{Bu})(\text{I}'\text{Bu}')$ (**3**; right), showing hydridic-to-protonic interactions.

commonly postulated intermediates en route to C–H bond activation, such species are difficult to detect. We are not aware of any examples where both the immediate precursors (i.e., the agostic complexes **2** and **3**) and the products of a C–H activation process (**4** and **5**) have been characterized by X-ray crystallography.²⁹ While the results here show that both rhodium and iridium undergo unique double cyclometalation processes, the ease with which these C–H activation processes take place is markedly different. Comparing reaction times for the transformation in benzene illustrates this point: 1 h (first cyclometalation) and 4 h (first and second) for rhodium, 20 h (first cyclometalation) and 120 h (first and second) for iridium. On the basis of available data on C–H reactivity of other Ir(III) compounds and the lack thereof for Rh(III) complexes, the results for the second cyclometalation step described here appear counterintuitive. In situ NMR experiments for both rhodium and iridium systems did not show buildup of intermediates during the second cyclometalation and preclude any meaningful discussion on possibly different mechanisms at work for the two metals (i.e., oxidative addition vs metathesis). On the contrary, analysis of the solid-state structures of **2** and **3** shows that there are close hydridic–protonic interactions between the hydride ligand in **2** and **3** and two of the hydrogen atoms of the second, nonagostic ^tBu group of I'Bu (Figure 3). The resulting M–H⋯H–C contacts with distances between 1.9 and 2.1 Å are considerably shorter than the sums of the van der Waals radii for H of 2.4 Å expected in the absence of attractive interactions.³⁰ Although unlikely, we therefore cannot exclude the possibility that the non-agostic ^tBu group is activated (through a mechanism involving initial proton transfer) and that the agostic bonds in **2** and **3** are merely rendering the metal center more susceptible to the second C–H activation process.

Isolation and Characterization of Bare 14-Electron Complexes. The addition of 1 equiv of AgPF_6 to **4** and **5** in CH_2Cl_2 leads to abstraction of the chloride ligand and formation of 14-electron complexes $[\text{Rh}(\text{I}'\text{Bu})_2]\text{PF}_6$ (**6**) and $[\text{Ir}(\text{I}'\text{Bu})_2]\text{PF}_6$ (**7**) according to eq 1. Workup provides the cationic complexes as



yellow-orange (**6**) and green-red (**7**) solids in high yield. Interestingly, the iridium complex **7** is also obtained directly

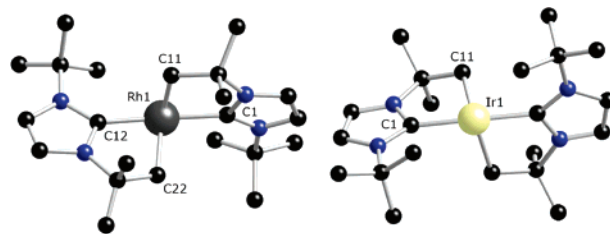


Figure 4. Ball-and-stick representations of complexes $[\text{Rh}(\text{I}'\text{Bu}')_2]\text{PF}_6$ (**6**; left) and $[\text{Ir}(\text{I}'\text{Bu}')_2]\text{PF}_6$ (**7**; right). Hydrogen atoms and PF_6^- omitted for clarity.

from the reaction of **3** with AgPF_6 in $\text{C}_6\text{H}_5\text{F}$, meaning that the initially formed cationic complex $[\text{IrH}(\text{I}'\text{Bu})(\text{I}'\text{Bu}')]\text{PF}_6$ undergoes a rapid second cyclometalation step to give **7** (overall reaction time 2 h).³² This result is not entirely unexpected, as it is known from studies employing $\text{Cp}^*\text{Ir}^{\text{III}}$ complexes that cationic species are substantially more prone to undergo C–H activation processes than their neutral analogues.³³

The 14-electron compounds **6** and **7** were fully characterized by elemental analysis, spectroscopic methods, and X-ray analyses. The ³¹P and ¹⁹F NMR spectra of **6** and **7** give resonances typical for the free PF_6^- counterion. The ¹H NMR spectrum shows characteristic signals for the metalated CH_2 groups [at 3.06 (d) and 2.39 (dd) ppm for **6**, at 4.10 (d) and 3.86 (d) ppm for **7**]. Three distinct resonances for the free CH_3 groups (intensity 3:1:1) and two sets of signals for the protons of the imidazole rings gave no indication of agostic interactions of the free ^tBu groups. The composition of **6** and **7** was confirmed by elemental analyses, and to unambiguously ascertain the exact structure of these complexes, X-ray-quality crystals were obtained by slow evaporation of a $\text{CH}_2\text{Cl}_2/\text{C}_6\text{H}_5\text{F}$ solution (for **6**) and by slow diffusion of diethyl ether into CH_2Cl_2 (for **7**). Their structures are shown in Figure 4, and important bond lengths and angles can be found in Table 3. Analogous to those of their neutral 16-electron counterparts **4** and **5**, the two carbenic carbon atoms are disposed in a mutually *trans* arrangement with their corresponding cyclometalated CH_2 groups *cis* with respect to each other. The geometry of these unique compounds is best described as highly distorted, divacant octahedral (Table 3). We note that although these highly electrophilic complexes have two empty coordination sites, they are stabilized neither by agostic interactions nor by a change in spin state as observed very recently by Caulton et al. for a Ru(II) compound.^{6b} In fact, the distances between the metal centers and the free ^tBu groups are outside the range for even weak agostic interactions.^{8,34} DFT calculations below give a convincing explanation for the stability of these bare 14-electron compounds.

(29) For an example of an agostic Ir complex showing reversible metalation, see: Albeniz, A. C.; Schulte, G.; Crabtree, R. H. *Organometallics* **1992**, *11*, 242–249.

(30) Related examples of proton–hydride interactions involve close contacts between iridium(III) hydrides and a hydrogen atom coordinated to an electronegative heteroatom (O, N). Proton transfer from these acidic hydrogens to Ir–H and formation of iridium dihydrogen complexes have been observed; see: (a) Lough, A. J.; Park, S.; Ramachandran, R.; Morris, R. H. *J. Am. Chem. Soc.* **1994**, *116*, 8356–8357. (b) Lee, J. C. Jr.; Peris, E.; Rheingold, A. L.; Crabtree, R. H. *J. Am. Chem. Soc.* **1994**, *116*, 11014–11019. For a review on proton–hydride interactions, see: (c) Custelcean, R.; Jackson, J. E. *Chem. Rev.* **2001**, *101*, 1963–1980.

(31) Several X-ray structures shown here appear as mirror images of each other. This is due to the fact that they are chiral at the metal center and that an inversion center is imposed upon refinement of their structures.

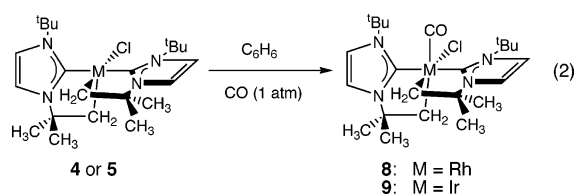
(32) In the rhodium case, we observe decomposition to several unidentified products.

(33) Tellers, D. M.; Yung, C. M.; Arndtsen, B. A.; Adamson, D. R.; Bergman, R. G. *J. Am. Chem. Soc.* **2002**, *124*, 1400–1410.

Table 3. Selected Bond Lengths (Å) and Angles (deg) for [Rh(I^tBu')₂]₂PF₆ (**6**), [Ir(I^tBu')₂]₂PF₆ (**7**), [Rh(I^tBu')₂(CO)₂]₂PF₆ (**10**), and [Ir(I^tBu')₂(CO)₂]₂PF₆ (**11**)

	6	7	10	11
M1–C1	2.049(6)	2.028(11)	2.079(5)	2.000(17)
M1–C5	2.014(6)	2.038(10)	2.092(6)	2.025(16)
M1–C12	2.015(6)	2.028(11)	2.079(5)	1.991(18)
M1–C16	2.014(5)	2.038(10)	2.106(6)	2.128(18)
M1–C23			1.956(7)	1.993(19)
M1–C24			2.017(8)	2.070(20)
C1–M1–C5	80.4(2)	79.4(4)	80.4(2)	78.1(8)
C1–M1–C16	96.5(2)	97.8(4)	87.9(2)	89.3(7)
C1–M1–C12	173.14(8)	175.0(5)	163.4(2)	160.2(8)
C5–M1–C12	95.7(3)	97.8(4)	87.2(2)	85.0(8)
C5–M1–C24			171.6(3)	173.7(9)
C16–M1–C23			175.0(2)	176.1(8)

Reactivity Studies of Complexes 4–7 with CO. The coordinatively unsaturated nature of the cationic 14-electron complexes **6** and **7**, and of their neutral 16-electron analogues **4** and **5**, offers an opportunity to examine whether a small linear molecule such as CO can simply add to these to generate six-coordinate saturated complexes and confirm, by analysis of structural differences, the unsaturated nature of the “precursor” complexes **4–7**. Indeed, complexes **4–7** react instantaneously with carbon monoxide. Treating a benzene solution of MCl(I^tBu')₂ (**4** or **5**) with 1 atm of CO results in rapid formation of the saturated RhCl(I^tBu')₂(CO) (**8**) and IrCl(I^tBu')₂(CO) (**9**) complexes that precipitate from solution as white solids in almost quantitative yield (eq 2).



Satisfactory elemental analysis confirmed the compositions of **8** and **9**. Infrared spectroscopy showed the presence of one terminal $\nu(\text{CO})$ band at 2015 cm^{-1} (**8**) and 1980 cm^{-1} (**9**), indicating efficient back-bonding to the carbonyls. ¹H and ¹³C NMR spectra of **8** and **9** in CD₂Cl₂ showed resonances characteristic of the cyclometalated I^tBu' ligands (i.e., two signals for the metalated CH₂ groups, two resonances for the free CH₃ groups, and two sets of signals for the protons of the imidazole rings). Coordination of CO in **8** and **9** was confirmed by an additional low-field signal in ¹³C NMR near 180 ppm. Colorless crystals of **8** and **9** suitable for X-ray diffraction were obtained by slow diffusion of hexane into a concentrated CH₂Cl₂ solution. The geometry around each metal center is that of a distorted octahedron (Figure 5). Analogous to those of complexes **4** and **5**, the two carbenic carbon atoms are disposed *trans* to each other with their corresponding cyclometalated CH₂ group *cis* with respect to each other but *trans* to either the carbonyl or the chloride group. The incoming CO occupies the previously vacant site. Consistent with an increase in steric congestion around the metal center, rationalized by simply having one more ligand present, the *trans* carbenic carbon atoms in **8** and **9** are perturbed from linearity when compared to those

(34) These do not give solvent–ligand adducts when dissolved in potentially coordinating solvents such as dichloromethane, THF, or acetone.

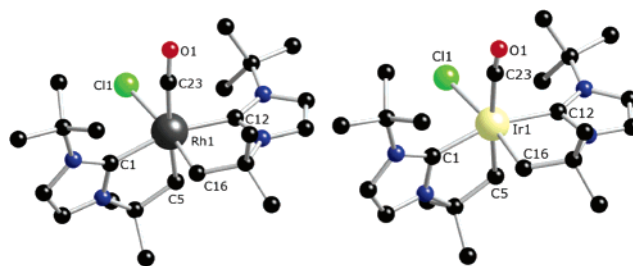


Figure 5. Ball-and-stick representations of complexes RhCl(I^tBu')₂(CO) (**8**; left) and IrCl(I^tBu')₂(CO) (**9**; right). Hydrogen atoms are omitted for clarity.

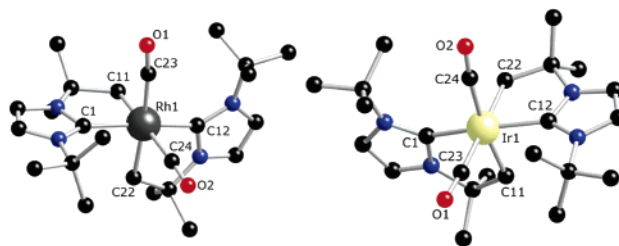
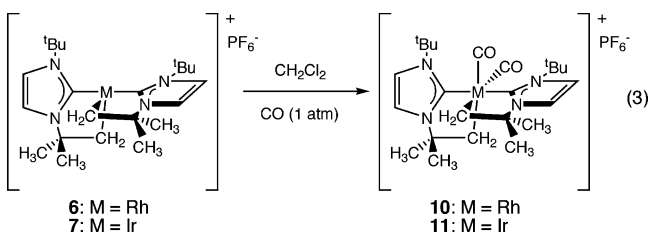


Figure 6. Ball-and-stick representations of complexes [Rh(I^tBu')₂(CO)₂]-PF₆ (**10**; left) and [Ir(I^tBu')₂(CO)₂]-PF₆ (**11**; right). Hydrogen atoms and PF₆[−] are omitted for clarity.

of complexes **4** or **5** (see Table 2). The metal bond distances of the cyclometalated carbons (C5, C12) are marginally longer for the same reason. While the Ir–Cl(1) distance of **9** is similar to that of **5**, the Rh–C11 bond length for **8** is considerably longer than the corresponding distance in **4**.

The reactivity of the 14-electron complexes [M(I^tBu')₂]₂PF₆ (**6**, **7**) toward CO showed the two vacant sites to be readily accessible, and the reaction proceeds by CO coordination of the empty sites only. Treating **6** or **7** with 1 atm of CO in CH₂Cl₂ afforded the colorless 18-electron complexes [Rh(I^tBu')₂(CO)₂]₂PF₆ (**10**) and [Ir(I^tBu')₂(CO)₂]₂PF₆ (**11**) in high yield according to eq 3.



IR data for **10** and **11** indicate that a dicarbonyl species is present, while the ¹³C NMR data show that the two carbonyl ligands are equivalent. ¹H NMR data for **10** and **11** give resonances characteristic of cyclometalated I^tBu' ligands. To establish the structure of these complexes and to permit a comparison with **6** and **7**, single-crystal diffraction studies were performed on **10** and **11** from colorless crystals obtained by slow diffusion of Et₂O over saturated CH₂Cl₂ solutions. These structures are shown in Figure 6, and bond lengths and angles are given in Table 3. Each molecule is monomeric with a six-coordinate octahedral metal center. The arrangement of the two cyclometalated I^tBu' ligands is very similar to that of **6** and **7** with two CO molecules now occupying the previously empty axial and equatorial positions. Although the I^tBu' environment remains essentially unperturbed with respect to that of **6** and **7**, marginal wing contractions in the butterfly-like structures are

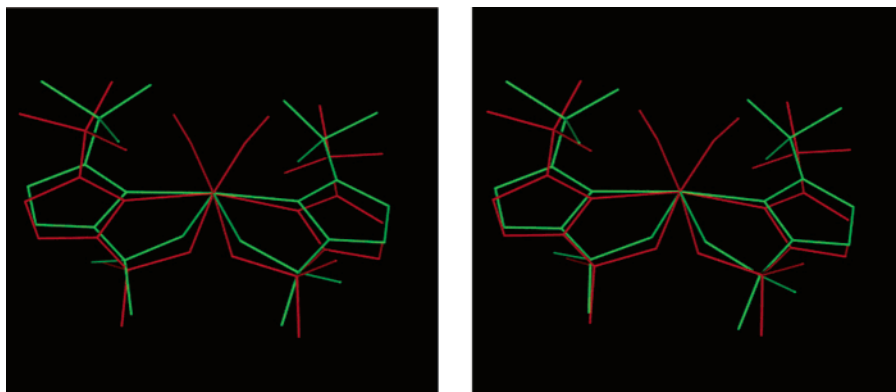


Figure 7. Overlap of the X-ray structures of $[\text{Rh}(\text{I}'\text{Bu}')_2]^+$ (**6**) with $[\text{Rh}(\text{I}'\text{Bu}')_2(\text{CO})_2]^+$ (**10**; left) and $[\text{Ir}(\text{I}'\text{Bu}')_2]^+$ (**7**) with $[\text{Ir}(\text{I}'\text{Bu}')_2(\text{CO})_2]^+$ (**11**; right).

observed $[\text{C1}-\text{M}-\text{C12}] =$ (**6**) $173.14(8)^\circ$, (**7**) $175.0(5)^\circ$, (**10**) $163.4(2)^\circ$, and (**11**) $160.2(8)^\circ$ due to the steric requirement of adding two ligands around the now six-coordinate complexes (see the structure-overlapping diagram in Figure 7). The small variations observed in the overlays lend further support to the unique nature of complexes **6** and **7**, and no further reactivity, such as CO insertion via migration of the metalated I'Bu' arms, is observed for complexes **10** and **11**. These compounds are rare examples of all-carbon-based octahedral Rh(III) and Ir(III) compounds. To the best of our knowledge, reported complexes of this type are limited to the homoleptic hexamethyl species $[\text{MMe}_6]^{3-}$ ($\text{M} = \text{Rh}, \text{Ir}$) and the hexacarbonyl compound $[\text{Ir}(\text{CO})_6]^{3+}$.³⁵

DFT Calculations on $\text{MCl}(\text{I}'\text{Bu}')_2$ and $[\text{M}(\text{I}'\text{Bu}')_2]\text{PF}_6$ Compounds. On a qualitative level, the unusual stability of complexes **6** and **7** might be attributed to the electron-donating nature of the all-carbon-based NHC ligands surrounding the metals, which renders them less electrophilic than the previously reported phosphine-containing 14-electron $d^6\text{-ML}_4$ compounds.³⁶ To paint a more detailed picture of the electronic situation in complexes **6** and **7**, we performed density functional theory (DFT) calculations on the $\text{MCl}(\text{I}'\text{Bu}')_2$ and $[\text{M}(\text{I}'\text{Bu}')_2]^+$ ($\text{M} = \text{Rh}, \text{Ir}$) fragments. For the sake of simplicity, we will limit our discussion to the Ir systems, but the calculations on the Rh systems lead to analogous conclusions.

First, we note that both the X-ray and the DFT-optimized structures of **5** present rather different Ir–C(carbene) bond lengths, the Ir–C(1) distance (X-ray, 1.982 Å; DFT, 1.988 Å) being roughly 0.1 Å shorter than the Ir–C(12) distance (X-ray, 2.103 Å; DFT, 2.108 Å). Since the two Ir–C(carbene) bonds are *trans* to each other, this asymmetry suggests a different bonding scheme between the two NHC ligands and the Ir atom. Natural bond order (NBO) analysis indicates that the bond order of the Ir–C(1) bond (0.62) is 0.11 greater than that of the Ir–C(12) bond (0.51). Molecular Orbital (MO) analysis suggests that the higher bond order of the shorter Ir–C(1) bond is due to a partial $\pi \rightarrow d$ donation from the filled π MO highest in energy of the NHC ligand to empty d MOs of the metal. The lowest unoccupied molecular orbital (LUMO) of **5**, shown in Figure 8, has a d_{z^2} character and is oriented along the empty coordination position of the octahedral Ir atom.

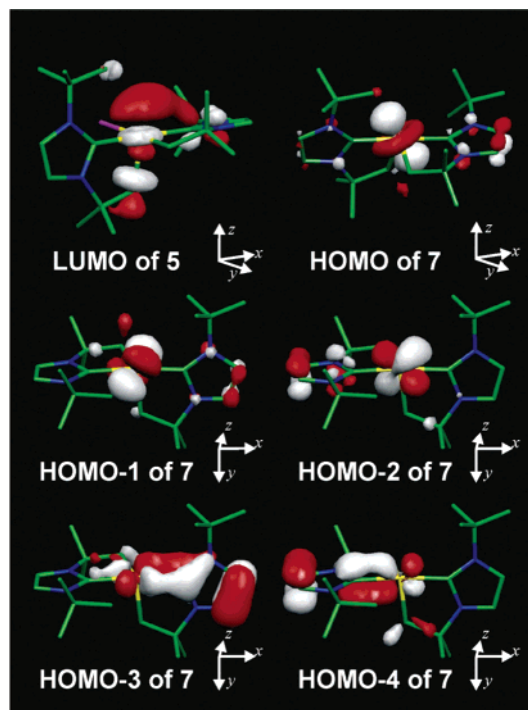


Figure 8. Most representative MOs of **5** and of **7**. Hydrogen atoms are omitted for clarity.

The MO situation in complex **7** is quite different. This complex is characterized by a local C_2 symmetry axis that bisects the two empty coordination positions and the two Ir–CH₂ bonds. The highest occupied molecular orbital (HOMO), shown in Figure 8, is oriented along the local C_2 symmetry axis, and has a strong d_{z^2} character. The HOMO – 1 and HOMO – 2 are a combination of d_{xz} and d_{yz} orbitals mainly, and are also shown in Figure 8. Finally, the HOMO – 3 and HOMO – 4 show a strong interaction between the filled π MO highest in energy of the NHC ligands and empty d orbitals of the metal.

To obtain further insights into the NHC–M bonding, we analyzed the model system **12** within C_2 symmetry. The optimized geometry of **12** is reported in Figure 9. Replacing the σ -bonding alkyl arm of I'Bu' with a simple CH₃ group allows the first BDE of the NHC to the Ir atom in **12** to be estimated, 65.4 kcal/mol. This value is comparable the NHC BDEs calculated by Meyer and co-workers for related cationic Cu, Ag, and Au complexes, 81.5, 55.2, and 76.2 kcal/mol, respectively.³⁷ The C_2 symmetry of **12** does not allow easy separation of σ and π contributions to the bonding energy. Nevertheless,

(35) (a) Hay-Motherwell, R. S.; Wilkinson, G.; Hussain, B.; Hursthouse, M. B. *J. Chem. Soc., Chem. Commun.* **1989**, 1436–1437. (b) von Ahsen, B.; Berkei, M.; Henkel, G.; Willner, H.; Aubke, F. *J. Am. Chem. Soc.* **2002**, *124*, 8371–8379.

(36) NHCs are better donor ligands than alkylphosphines; see ref 13.

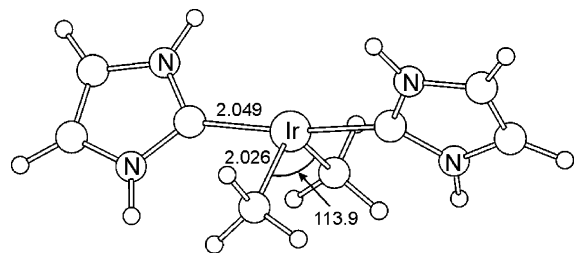


Figure 9. DFT-optimized geometry of **12**.

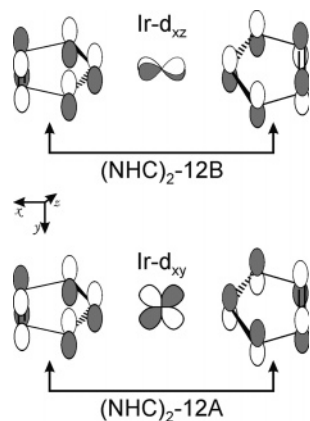


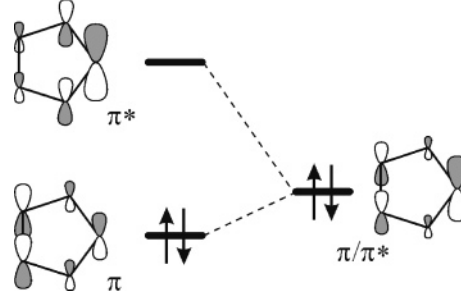
Figure 10. Qualitative representation of the interactions between π MOs of the $(\text{NHC})_2$ fragment and the d MO of the $[\text{Ir}(\text{Me})_2]^+$ fragment of **12**.

the bonding between the two NHC fragments and the metal can be rationalized with qualitative MO analysis. Linear combination of the filled and highest in energy π MOs of the NHC fragments results in the π MOs 12A and 12B of Figure 10.³⁸ The filled π 12A MO strongly interacts with the d_{xy} MO of the metal fragment. The 12A– d_{xy} interaction is further stabilized by mixing of empty π^* MOs of the NHC fragments. Mixing of this empty MO, depicted in Scheme 2 for a single NHC ligand, substantially localizes electron density on the carbene C atom of the NHC ligand, enhancing the π donor properties of the NHC ligands. The composition of the resulting MO of the complex is 64% 12A and 28% d_{xy} , while the above-mentioned π^* MO of the NHC fragments contributes 3%. Conversely, the filled π 12B MO interacts less efficiently with the mainly d_{xz} MO of the metal fragment; see Figure 10. The less efficient B symmetric 12B– d_{xy} interaction results in an MO of the complex with the following composition: 80% 12B and 9% d_{xz} .

The MO analysis indicates that *the ability of NHC ligands to act as π -electron donors is key in understanding the unusual stability of the 14-electron complexes **6** and **7***. In fact, there are two reservoirs of electron density that can be donated to alleviate the electron deficiency on the metal: the π orbital of the NHCs and the σ orbitals of the C–H bonds of the ^tBu groups. Our analysis shows clearly that, in the present case, the π orbital of the NHC ligand is preferred over the σ orbital of the C–H bond, and this explains both the absence of agostic interactions in **6** and **7** and their remarkable stability.

This analysis illustrates that NHC ligands are electronically much more flexible than commonly thought (simple σ donors), since the π orbitals on the NHC ring can be deeply involved in

Scheme 2. Mixing of Empty NHC Molecular Orbitals



the bonding to the metal. For instance, recent results by Meyer and co-workers nicely indicated that NHC can accept electron density from electron-rich metal atoms, through a $d \rightarrow \pi^*$ back-donation scheme.³⁷ Our analysis broadens further the bonding ability of NHC ligands, since it suggests that they can also donate electron density to electron-poor metal atoms, through a $\pi \rightarrow d$ donation scheme. Stabilization of this kind might have important implications in catalysis. Slower decomposition of the catalytically active, highly unsaturated species normally involved in catalysis could be the reason LTM–NHC compounds often display higher thermal stability when compared to analogous LTM– PR_3 systems. As an example, the active species in ruthenium-catalyzed metathesis reactions, $\text{RuCl}_2(\text{L})(=\text{CHPh})$ ($\text{L} = \text{PR}_3$ or NHC), has the same electronic configuration as complexes **6** and **7** and might be stabilized more efficiently through similar $\pi(\text{NHC})\text{--}d(\text{LTM})$ donations.

Conclusions

We have described the interaction of the bulky *N*-heterocyclic carbene ligand ^tBu with the neutral Rh(I) and Ir(I) precursors $[\text{M}(\text{COE})_2\text{Cl}]_2$ using 2 equiv of ^tBu per metal center. Initial replacement of the cyclooctene ligands by the NHCs is followed by a unique double cyclometalation process of both ^tBu ligands. We were able to isolate and fully characterize the resulting M(III) complexes of formula $\text{MCl}(\text{I}^t\text{Bu})_2$. By a simple change of solvent (for Rh) or of reaction times (for Ir), we obtained several precursors, most notably the hydride complexes arising from the first intramolecular C–H activation step, namely, $\text{MClH}(\text{I}^t\text{Bu})(\text{I}^t\text{Bu}')$. Abstraction of the chloride ligand from neutral and unsaturated complexes $\text{MCl}(\text{I}^t\text{Bu})_2$ enabled the isolation of the first examples of “bare” 14-electron complexes $[\text{Rh}(\text{I}^t\text{Bu})_2]\text{PF}_6$ and $[\text{Ir}(\text{I}^t\text{Bu})_2]\text{PF}_6$. Not only are stabilizing agostic interactions absent in these homoleptic complexes, but they also do not form metal–ligand adducts with σ -donor ligands such as acetone or THF. However, they do interact readily with CO to give the saturated complexes $[\text{M}(\text{I}^t\text{Bu})_2(\text{CO})_2]\text{PF}_6$, which represent rare examples of octahedral, all-carbon-bound organometallic species. Finally, DFT calculations on both the 16-electron and 14-electron complexes reveal an important new aspect in the bonding interaction of the *N*-heterocyclic carbene ligand class with metal centers. Whereas NHCs have normally been considered as pure σ -donor ligands, they can also donate electron density through $\pi \rightarrow d$ interactions, and we show here that the π -donor ability of NHCs is crucial in understanding the remarkable stability as well as the lack of agostic interactions in the 14-electron $[\text{M}(\text{I}^t\text{Bu})_2]\text{PF}_6$ compounds.

Whether the reactivity profile seen here is limited to ^tBu is presently being examined in our laboratories. The ease of intramolecular C–H activation as well as the new bonding

(37) Hu, X.; Castro-Rodriguez, I.; Olsen, K.; Meyer, K. *Organometallics* **2004**, *23*, 755–764.

(38) The MO numbering follows the ADF output.

aspects of NHCs described here might also open new prospects for the activation and functionalization of external substrates. These exciting possibilities are currently being explored.

Experimental Section

General Considerations. All reactions were carried out using standard Schlenk techniques under an atmosphere of dry argon or in an MBraun glovebox containing dry argon. Solvents were distilled from appropriate drying agents or were passed through an alumina column in an MBraun solvent purification system. Other anhydrous solvents were purchased from Aldrich, degassed prior to use by purging with dry argon, and kept over molecular sieves. Solvents for NMR spectroscopy were degassed with argon and dried over molecular sieves. Experiments involving silver salts were carried out in the dark. NMR spectra were collected on 300, 400, or 500 MHz Varian Gemini spectrometers. Elemental analyses were performed by Robertson Microlit Laboratories, Madison, NJ. $[\text{Rh}(\text{COE})_2\text{Cl}]_2$ ³⁹ and $[\text{Ir}(\text{COE})_2\text{Cl}]_2$ ⁴⁰ were synthesized following literature procedures. The free carbene tBu (*N,N*-di(*tert*-butyl)imidazol-2-ylidene) was synthesized according to an adaptation of the literature procedure.⁴¹

Synthesis of $\text{tBu}\cdot\text{HBF}_4$. To a stirring solution of toluene (200 mL) and paraformaldehyde (6.00 g, 0.20 mol) in a two-necked round-bottom flask at 0 °C was added dropwise *tert*-butylamine (29.26 g, 0.40 mol) over 20 min. The reaction mixture was stirred for a further 5 min, and then 50 mL of HCl (4 N in dioxane) was added slowly. After the reaction reached completion (no longer exothermic), the mixture was allowed to warm to room temperature, and glyoxal (40 wt %, 29.02 g, 0.20 mol) was slowly added. The resulting mixture was stirred at 25 °C for 12 h. The solution was then degassed with argon (15 min), and under argon the solvent volume was concentrated almost to dryness via slow distillation by heating the reaction mixture to 105 °C for 4 h. The reaction mixture was cooled to 50 °C, and the remaining solvent was removed under vacuum. The resulting brown solid ($\text{tBu}\cdot\text{HCl}$) was dissolved in water (150 mL) and filtered, and HBF_4 (0.20 mol) was added to the solution to afford a white precipitate ($\text{tBu}\cdot\text{HBF}_4$). The white solid was filtered, washed with water (3 × 20 mL), and then dried under vacuum. Yield: 39.60 g (65%). ¹H NMR (CDCl_3): δ = 8.83 (s, 1H, $\text{tBu}\cdot\text{HBF}_4$), 7.46 (s, 2H, *CH*-imidazole), 1.72 (s, 18H, C^{tBu}).

Synthesis of tBu . In a drybox $\text{tBu}\cdot\text{HBF}_4$ (8.65 g, 29.0 mmol), NaH (1.38 g, 58.0 mmol), and a catalytic amount of KO^{tBu} (100 mg) were loaded into a flask. Tetrahydrofuran (125 mL) was added to the flask, and the resulting mixture was stirred for 12 h. The solvent was removed under vacuum, and the resulting solid was transferred to a sublimation apparatus. tBu was sublimed under static vacuum with slight heating to afford a white crystalline product. Yield: 2.52 g, (41%). ¹H NMR (C_6D_6): δ = 7.56 (s, 2H, *CH*-imidazole), 1.89 (s, 18H, C^{tBu}).

Synthesis of $[\text{Rh}(\text{COE})(\text{tBu})\text{Cl}]_2$ (1**).** To a yellow pentane slurry (130 mL) of $[\text{Rh}(\text{COE})_2\text{Cl}]_2$ (600 mg, 0.836 mmol) was added dropwise a pentane solution (20 mL) of tBu (627 mg, 3.478 mmol). Stirring at room temperature for 10 min afforded a limpid yellow solution. Continued stirring led to the precipitation of a pale yellow solid after 30 min. After being stirring for another 30 min, the suspension was decanted⁴² and the solid washed with additional pentane (3 × 10 mL) and dried in vacuo. Yield: 595 mg (83%). ¹H NMR (C_6D_6): δ = 6.53 (s, 2H, *CH*-imidazole), 2.61 (br, 2H, *CH*-olefin), 2.20–2.43 (2 br, 4H, CH_2 -olefin), 2.17 (s, 18H, $\text{C}(\text{CH}_3)_3$), 1.40–1.78 (several br, 8H, CH_2 -olefin). ¹³C NMR (C_6D_6): δ = 178.30 (d, $J_{\text{Rh-C}}$ = 56.9 Hz, *C*-carbene), 119.89 (s, *CH*-imidazole), 59.45 (s, C^{tBu}), 58.51 (d, $J_{\text{Rh-C}}$ = 18.1 Hz,

CH-olefin), 33.55 (s, $\text{C}(\text{CH}_3)_3$), 31.23 (s, CH_2 -olefin), 29.99 (s, CH_2 -olefin), 27.34 (s, CH_2 -olefin). Anal. Calcd for $\text{C}_{38}\text{H}_{68}\text{Cl}_2\text{N}_4\text{Rh}_2$ (857.70): C, 53.21; H, 7.99; N, 6.53. Found: C, 53.12; H, 8.29; N, 6.29.

Synthesis of $\text{RhCl}(\text{tBu})(\text{tBu}')$ (2**).** A hexane solution (10 mL) of tBu (315 mg, 1.742 mmol) was added dropwise under stirring to a yellow hexane slurry (60 mL) of $[\text{Rh}(\text{COE})_2\text{Cl}]_2$ (300 mg, 0.418 mmol). The resulting yellow solution was stirred at room temperature for 4 h and then concentrated to ca. 1/3 of its volume.⁴³ The partially formed yellow precipitate was treated with pentane (40 mL), leading to further precipitation. The supernatant solution was decanted and the solid washed with pentane (3 × 5 mL) and dried in vacuo. Yield: 379 mg (91%). ¹H NMR (C_6D_6): δ = 6.74 (d, J = 1.8 Hz, 1H, *CH*-imidazole), 6.59 (br, 2H, *CH*-imidazole), 6.46 (d, J = 1.8 Hz, 1H, *CH*-imidazole), ca. 2.1 (overlapped, 2H, $\text{C}(\text{CH}_3)_2\text{CH}_2$), 2.03 (s, 9H, $\text{C}(\text{CH}_3)_3$), 1.64 (br, 18H, $\text{C}(\text{CH}_3)_3$), 1.36 (s, 6H, $\text{C}(\text{CH}_3)_2\text{CH}_2$), –22.93 (br, 1H, *RhH*). ¹³C NMR (C_6D_6): δ = 186.14 (d, $J_{\text{Rh-C}}$ = 44.9 Hz, *C*-carbene), 179.91 (d, $J_{\text{Rh-C}}$ = 39.6 Hz, *C*-carbene), 118.59 (s, *CH*-imidazole), 114.48 (s, *CH*-imidazole), 64.84 (s, C^{tBu}), 58.89 (s, C^{tBu}), 32.01 (s, $\text{C}(\text{CH}_3)_3$), 31.73 (s, $\text{C}(\text{CH}_3)_2\text{CH}_2$), 28.26 (d, $J_{\text{Rh-C}}$ = 28.9 Hz, $\text{C}(\text{CH}_3)_2\text{CH}_2$). Anal. Calcd for $\text{C}_{22}\text{H}_{40}\text{ClN}_4\text{Rh}$ (498.93): C, 52.96; H, 8.08; N, 11.23. Found: C, 53.12; H, 8.23; N, 10.83.

Synthesis of $\text{IrCl}(\text{tBu})(\text{tBu}')$ (3**).** A benzene solution (3 mL) of tBu (330 mg, 1.830 mmol) was added dropwise under stirring to an orange benzene slurry (5 mL) of $[\text{Ir}(\text{COE})_2\text{Cl}]_2$ (395 mg, 0.440 mmol). The resulting yellow-orange solution was stirred at room temperature for 20 h and then concentrated to ca. 1/3 of its volume. The partially formed yellow precipitate was treated with pentane (10 mL), leading to further precipitation. The supernatant solution was decanted and the solid washed with pentane (3 × 5 mL) and dried in vacuo. Yield: 471 mg (91%). ¹H NMR (C_6D_6): δ = 6.78 (s, 1H, *CH*-imidazole), 6.69 (s, 1H, *CH*-imidazole), 6.49 (s, 1H, *CH*-imidazole), 6.41 (s, 1H, *CH*-imidazole), 2.55 (d, J = 11.6 Hz, 1H, $\text{C}(\text{CH}_3)_2\text{CH}_2$), 2.42 (d, J = 10.8 Hz, 1H, $\text{C}(\text{CH}_3)_2\text{CH}_2$), 2.01 (s, 9H, $\text{C}(\text{CH}_3)_3$), 1.82 (s, 9H, $\text{C}(\text{CH}_3)_3$), 1.42 (s, 3H, $\text{C}(\text{CH}_3)_2\text{CH}_2$), 1.32 (s, 3H, $\text{C}(\text{CH}_3)_2\text{CH}_2$), 1.15 (s, 9H, $\text{C}(\text{CH}_3)_3$), –32.83 (s, 1H, *IrH*). ¹³C NMR (C_6D_6): δ = 177.11 (s, *C*-carbene), 167.78 (s, *C*-carbene), 118.23 (s, *CH*-imidazole), 118.13 (s, *CH*-imidazole), 115.82 (s, *CH*-imidazole), 114.43 (s, *CH*-imidazole), 65.07 (s, C^{tBu}), 59.55 (s, C^{tBu}), 58.83 (s, C^{tBu}), 57.79 (s, C^{tBu}), 31.83 (s, $\text{C}(\text{CH}_3)_3$), 31.56 (s, $\text{C}(\text{CH}_3)_3$), 31.41 (s, $\text{C}(\text{CH}_3)_2\text{CH}_2$), 30.70 (s, $\text{C}(\text{CH}_3)_2\text{CH}_2$), 29.96 (s, $\text{C}(\text{CH}_3)_3$), 9.49 (s, $\text{C}(\text{CH}_3)_2\text{CH}_2$). Anal. Calcd for $\text{C}_{22}\text{H}_{40}\text{ClN}_4\text{Ir}$ (588.26): C, 44.92; H, 6.85; N, 9.52. Found: C, 45.29; H, 6.83; N, 9.35.

Synthesis of $\text{RhCl}(\text{tBu})_2$ (4**).** A benzene solution (10 mL) of tBu (315 mg, 1.742 mmol) was added dropwise under stirring to a yellow benzene solution (10 mL) of $[\text{Rh}(\text{COE})_2\text{Cl}]_2$ (300 mg, 0.418 mmol). The resulting solution was stirred at room temperature for 4 h, giving a dark orange solution which was subsequently concentrated to ca. 3 mL. Addition of pentane (15 mL) led to the precipitation of a yellow solid which was washed with pentane (3 × 5 mL) and dried in vacuo. Yield: 364 mg (88%). ¹H NMR (C_6D_6): δ = 6.61 (d, J = 2.0 Hz, 2H, *CH*-imidazole), 6.42 (d, J = 2.0 Hz, 2H, *CH*-imidazole), 2.92 (dd, J = 9 Hz and 4 Hz, 2H, $\text{C}(\text{CH}_3)_2\text{CH}_2$), 2.21 (d, J = 9.5 Hz, 2H, $\text{C}(\text{CH}_3)_2\text{CH}_2$), 1.77 (s, 18H, $\text{C}(\text{CH}_3)_3$), 1.40 (s, 6H, $\text{C}(\text{CH}_3)_2\text{CH}_2$), 1.28 (s, 6H, $\text{C}(\text{CH}_3)_2\text{CH}_2$). ¹³C NMR (C_6D_6): δ = 185.43 (d, $J_{\text{Rh-C}}$ = 43.1 Hz, *C*-carbenes), 117.46 (s, *CH*-imidazole), 114.82 (s, *CH*-imidazole), 64.87 (s, C^{tBu}), 58.12 (s, C^{tBu}), 32.45 (s, $\text{C}(\text{CH}_3)_2\text{CH}_2$), 31.53 (s, $\text{C}(\text{CH}_3)_2\text{CH}_2$), 31.46 (s, $\text{C}(\text{CH}_3)_3$), 28.97 (d, $J_{\text{Rh-C}}$ = 34.7 Hz, $\text{C}(\text{CH}_3)_2\text{CH}_2$). Anal. Calcd for $\text{C}_{22}\text{H}_{38}\text{ClN}_4\text{Rh}$ (496.92): C, 53.17; H, 7.71; N, 11.27. Found: C, 53.48; H, 8.14; N, 11.13.

Synthesis of $\text{IrCl}(\text{tBu})_2$ (5**) from **3**.** A benzene solution (18 mL) of $\text{IrCl}(\text{tBu})(\text{tBu}')$ (**3**) (180 mg, 0.306 mmol) was stirred vigorously at room temperature for 4 days. During this period, the reaction flask was opened to argon twice a day to evacuate the dihydrogen formed.

(39) Hofmann, P.; Meier, C.; Englert, U.; Schmidt, U. *Chem. Ber.* **1992**, *125*, 353–359.

(40) Herde, J. L.; Lambert, J. C.; Senoff, C. V. *Inorg. Synth.* **1974**, *15*, 19–20.

(41) Viciu, M. S.; Navarro, O.; Germaneau, R. F.; Kelly, R. K., III; Sommer, W.; Marion, N.; Stevens, E. D.; Cavallo, L.; Nolan, S. P. *Organometallics* **2004**, *23*, 1629–1635.

(42) Evaporation and analysis of the mother liquor show formation of **2** (in addition to free ligand and traces of **1**).

(43) Leaving the solution at room temperature for 3 days and subsequent workup result in a mixture of **2** (major) and **4** (minor).

The resulting, dark red solution was subsequently concentrated to ca. 4 mL. Addition of pentane (10 mL) led to the precipitation of a deep red solid which was washed with pentane (3 × 5 mL) and dried in vacuo. Yield: 172 mg (96%). ¹H NMR (C₆D₆): δ = 6.69 (s, 2H, CH-imidazole), 6.44 (s, 2H, CH-imidazole), 3.43 (d, *J* = 10.5 Hz, 2H, C(CH₃)₂CH₂), 3.03 (d, *J* = 10.0 Hz, 2H, C(CH₃)₂CH₂), 1.72 (s, 18H, C(CH₃)₃), 1.40 (s, 6H, C(CH₃)₂CH₂), 1.31 (s, 6H, C(CH₃)₂CH₂). ¹³C NMR (C₆D₆): δ = 179.88 (s, C-carbenes), 117.97 (s, CH-imidazole), 115.07 (s, CH-imidazole), 65.74 (s, C^tBu), 58.63 (s, C^tBu), 32.85 (s, C(CH₃)₂CH₂), 32.04 (s, C(CH₃)₂CH₂), 31.60 (s, C(CH₃)₃), 8.92 (s, C(CH₃)₂CH₂). Anal. Calcd for C₂₂H₃₈C₁₄N₄Ir (586.24): C, 45.07; H, 6.53; N, 9.56. Found: C, 45.18; H, 6.68; N, 9.22.

Direct Synthesis of 5. A benzene solution (10 mL) of tBu (600 mg, 3.328 mmol) was added dropwise under stirring to an orange benzene solution (50 mL) of [Ir(COE)₂Cl]₂ (774 mg, 0.800 mmol). The resulting solution was vigorously stirred at room temperature for 5 days, giving a dark red solution. During this time, the reaction flask was open to argon from time to time to evacuate the H₂ formed. The solution was subsequently concentrated to ca. 8 mL. Addition of pentane (20 mL) led to the precipitation of a deep red solid which was washed with pentane (3 × 10 mL) and dried in vacuo. Yield: 825 mg (88%).

Synthesis of [Rh(tBu')₂]PF₆ (6). To a yellow dichloromethane solution (20 mL) containing 4 (200 mg, 0.404 mmol) was added dropwise a dichloromethane solution (20 mL) of AgPF₆ (102 mg, 0.404 mmol). Stirring at room temperature for 35 min was followed by filtration of the AgCl salt over cotton/Celite. The filtered solution was concentrated to ca. 4 mL and precipitated with benzene (4 mL) and pentane (12 mL). The resulting yellow-orange solid was decanted and dried in vacuo. Yield: 227 mg (93%). ¹H NMR (CD₂Cl₂): δ = 7.26 (d, *J* = 2.0 Hz, 2H, CH-imidazole), 7.12 (s, *J* = 2.0 Hz, 2H, CH-imidazole), 3.07 (d, *J* = 10.0 Hz, 2H, C(CH₃)₂CH₂), 2.39 (dd, *J* = 9.6 and 4.8 Hz, 2H, C(CH₃)₂CH₂), 1.62 (s, 18H, C(CH₃)₃), 1.51 (s, 6H, C(CH₃)₂CH₂), 1.40 (s, 6H, C(CH₃)₂CH₂). ³¹P NMR (CD₂Cl₂): δ = -138.44 (septet, *J* = 711.5 Hz). ¹⁹F NMR (CD₂Cl₂): δ = 25.7 and 23.9 (*J* = 711.2 Hz). ¹³C NMR (CD₂Cl₂): δ = 181.82 (d, *J*_{Rh-C} = 44.9 Hz, C-carbenes), 119.33 (s, CH-imidazole), 117.27 (s, CH-imidazole), 67.51 (s, C^tBu), 58.54 (s, C^tBu), 32.12 (s), 32.01 (s, C(CH₃)₃), 29.92 (s), 29.62 (d, *J*_{Rh-C} = 39.5 Hz, C(CH₃)₂CH₂), 28.58 (s). Anal. Calcd for C₂₂H₃₈F₆N₄Pr (606.43): C, 43.57; H, 6.32; N, 9.24. Found: C, 43.28; H, 6.43; N, 9.15.

Synthesis of [Ir(tBu')₂]PF₆ (7) from Complex 3. To a yellow fluorobenzene solution (8 mL) containing 3 (80 mg, 0.136 mmol) was added dropwise a fluorobenzene solution (8 mL) of AgPF₆ (34 mg, 0.341 mmol). Stirring at room temperature for 90 min was followed by filtration of the AgCl salt over cotton/Celite. The filtered solution was concentrated to ca. 2 mL and precipitated with pentane (10 mL). The resulting red-brown solid was decanted, washed with pentane (2 × 3 mL), and dried in vacuo, giving a red-green solid. Yield: 75 mg (79%). ¹H NMR (CD₂Cl₂): δ = 7.42 (d, *J* = 1.8 Hz, 2H, CH-imidazole), 7.19 (s, *J* = 1.8 Hz, 2H, CH-imidazole), 4.10 (d, *J* = 11.4 Hz, 2H, C(CH₃)₂CH₂), 3.86 (d, *J* = 11.1, 2H, C(CH₃)₂CH₂), 1.58 (s, 18H, C(CH₃)₃), 1.50 (s, 6H, C(CH₃)₂CH₂), 1.33 (s, 6H, C(CH₃)₂CH₂). ³¹P NMR (CD₂Cl₂): δ = -143.40 (septet, *J* = 708.6 Hz). ¹⁹F NMR (CD₂Cl₂): δ = -72.55 and -75.06 (*J* = 708.2 Hz). ¹³C NMR (CD₂Cl₂): δ = 184.85 (s, C-carbenes), 119.97 (s, CH-imidazole), 116.80 (s, CH-imidazole), 68.79 (s, C^tBu), 58.88 (s, C^tBu), 32.86 (s), 32.05 (s, C(CH₃)₃), 25.32 (s), 8.22 (s, C(CH₃)₂CH₂). Anal. Calcd for C₂₂H₃₈F₆N₄Pr (695.75): C, 37.98; H, 5.51; N, 8.05. Found: C, 37.73; H, 5.46; N, 7.70.

Synthesis of 7 from Complex 5. To a yellow dichloromethane solution (6 mL) containing 5 (200 mg, 0.341 mmol) was added dropwise a dichloromethane solution (6 mL) of AgPF₆ (86 mg, 0.341 mmol). Stirring at room temperature for 40 min was followed by filtration of the AgCl salt over cotton/Celite. The filtered solution was concentrated to ca. 1 mL and precipitated with pentane (12 mL). The resulting red-

brown solid was decanted, washed with pentane (2 × 5 mL), and dried in vacuo, giving a red-green solid. Yield: 205 mg (86%).

Synthesis of RhCl(tBu')₂(CO) (8). A 50 mL flask was charged with 200 mg (0.402 mmol) of RhCl(tBu')₂ and 20 mL of benzene in the glovebox. The flask was taken out of the box and connected to a Schlenk line. The clear orange solution was purged with CO at room temperature for 5 min, after which the solvent was removed under vacuum. The residue was washed with pentane (2 × 5 mL), filtered, and dried in vacuo to afford a white powder. Yield: 180 mg (85%). ¹H NMR (CD₂Cl₂): δ = 7.17 (s, 1H, CH-imidazole), 7.10 (s, 1H, CH-imidazole), 6.88 (s, 1H, CH-imidazole), 6.82 (s, 1H, CH-imidazole), 2.60 (d, *J* = 10.0 Hz, 2H, C(CH₃)₂CH₂), 1.93 (dd, *J* = 11.5, 2H, C(CH₃)₂CH₂), 1.86 (s, 9H, C(CH₃)₃), 1.83 (s, 9H, C(CH₃)₃), 1.77 (s, 6H, C(CH₃)₂CH₂), 1.51 (3H, C(CH₃)₂CH₂), 1.27 (3H, C(CH₃)₂CH₂). ¹³C NMR (CD₂Cl₂): δ = 192.07 (d, *J*_{Rh-C} = 43.5 Hz, CO), 177.26 (d, *J*_{Rh-C} = 42 Hz, C-carbene), 173.50 (d, *J*_{Rh-C} = 41 Hz, C-carbene), 119.70 (s, CH-imidazole), 118.66 (s, CH-imidazole), 116.04 (s, CH-imidazole), 115.67 (s, CH-imidazole), 65.32 (s, C^tBu), 64.40 (s, C(CH₃)₂CH₂), 59.21 (s, C^tBu), 58.14 (s, C(CH₃)₂CH₂), 34.52 (s, C(CH₃)₂CH₂), 32.15 (s, C(CH₃)₂CH₂), 31.10 (s, C(CH₃)₃), 30.55 (s, C(CH₃)₃), 29.95 (d, *J*_{Rh-C} = 32.5 Hz, C(CH₃)₂CH₂). IR (CH₂Cl₂): ν(CO) 2015 cm⁻¹. Anal. Calcd for C₂₃H₃₈C₁₄N₄ORh (524.93): C, 52.63; H, 7.30; N, 10.67. Found: C, 52.31; H, 7.33; N, 10.23.

Synthesis of IrCl(tBu')₂(CO) (9). A 50 mL flask was charged with 86 mg (0.150 mmol) of IrCl(tBu')₂ and 20 mL of benzene in the glovebox. The flask was taken out of the box and connected to a Schlenk line. The clear red solution was purged with CO at room temperature for 5 min, after which the solvent was removed under vacuum. The residue was washed with pentane (2 × 5 mL), filtered, and dried in vacuo to afford a white powder. Yield: 75 mg (83%). ¹H NMR (CD₂Cl₂): δ = 7.21 (d, *J* = 2.0 Hz, 1H, CH-imidazole), 7.07 (d, *J* = 1.6 Hz, 1H, CH-imidazole), 6.86 (d, *J* = 2.0 Hz, 1H, CH-imidazole), 6.78 (d, *J* = 1.6 Hz, 1H, CH-imidazole), 2.47 (d, *J* = 11.5 Hz, 2H, C(CH₃)₂CH₂), 2.20 (d, *J* = 10.5, 2H, C(CH₃)₂CH₂), 1.86 (s, 9H, C(CH₃)₃), 1.83 (s, 9H, C(CH₃)₃), 1.55 (3H, C(CH₃)₂CH₂), 1.49 (3H, C(CH₃)₂CH₂), 1.45 (s, 3H, C(CH₃)₂CH₂), 1.22 (3H, C(CH₃)₂CH₂). ¹³C NMR (CD₂Cl₂): δ = 179.29 (s, CO), 162.20 (s, C-carbene), 154.77 (s, C-carbene), 119.63 (s, CH-imidazole), 118.51 (s, CH-imidazole), 116.62 (s, CH-imidazole), 115.70 (s, CH-imidazole), 65.06 (s, C^tBu), 64.74 (s, C(CH₃)₂CH₂), 59.45 (s, C^tBu), 58.45 (s, C(CH₃)₂CH₂), 35.51 (s, C(CH₃)₂CH₂), 35.14 (s, C(CH₃)₂CH₂), 31.90 (s, C(CH₃)₃), 31.50 (s, C(CH₃)₃), 13.99 (s, C(CH₃)₂CH₂). IR (CH₂Cl₂): ν(CO) 1980 cm⁻¹. Anal. Calcd for C₂₃H₃₈C₁₄N₄OIr (614.24): C, 44.97; H, 6.23; N, 9.12. Found: C, 45.18; H, 6.69; N, 9.22.

Synthesis of [Rh(tBu')₂(CO)₂]PF₆ (10). A 50 mL flask was charged with 100 mg (0.165 mmol) of [Rh(tBu')₂]PF₆ and 20 mL of dichloromethane in a glovebox. The flask was taken out of the box and connected to a Schlenk line. The clear red solution was purged with CO at room temperature for 5 min, after which the solvent was removed under vacuum. The residue was washed with pentane (2 × 5 mL), filtered, and dried in vacuo to afford a white powder. Yield: 89 mg (82%). ¹H NMR (CD₂Cl₂): δ = 7.32 (d, *J* = 2.0 Hz, 2H, CH-imidazole), 7.06 (d, *J* = 2.0 Hz, 2H, CH-imidazole), 2.30 (d, *J* = 10.9 Hz, 2H, C(CH₃)₂CH₂), 2.00 (d, *J* = 10.5 Hz, 2H, C(CH₃)₂CH₂), 1.79 (s, 18H, C(CH₃)₃), 1.63 (s, 6H, C(CH₃)₂CH₂), 1.41 (s, 6H, C(CH₃)₂CH₂). ³¹P NMR (CD₂Cl₂): δ = -138.13 (septet, *J* = 711.0 Hz). ¹⁹F NMR (CD₂Cl₂): δ = 25.89 and 24.00 (*J* = 710.4 Hz). ¹³C NMR (CD₂Cl₂): δ = 185.57 (br, CO), 162.71 (d, *J*_{Rh-C} = 40.0 Hz, C-carbenes), 121.69 (s, CH-imidazole), 118.18 (s, CH-imidazole), 65.14 (s, C^tBu), 58.83 (s, C(CH₃)₂CH₂), 33.24 (d, *J*_{Rh-C} = 28.0 Hz, C(CH₃)₂CH₂), 31.26 (s, C(CH₃)₃), 29.95 (s, C(CH₃)₂CH₂). IR (CH₂Cl₂): ν(CO) 2093, 2058 cm⁻¹. Anal. Calcd for C₂₄H₃₈F₆N₄O₂PRh (662.45): C, 43.51; H, 5.78; N, 8.46. Found: C, 43.50; H, 5.73; N, 8.14.

Synthesis of [Ir(tBu')₂(CO)₂]PF₆ (11). A 50 mL flask was charged with 100 mg (0.144 mmol) of [Ir(tBu')₂]PF₆ and 20 mL of dichloromethane in the glovebox. The flask was taken out of the box and

connected to a Schlenk line. The clear red solution was purged with CO at room temperature for 5 min, after which the solvent was removed under vacuum. The residue was washed with pentane (2×5 mL), filtered, and dried in vacuo to afford a white powder. Yield: 86 mg (79%). ^1H NMR (CD_2Cl_2): $\delta = 7.32$ (d, $J = 2.0$ Hz, 2H, CH-imidazole), 7.04 (d, $J = 2.0$ Hz, 2H, CH-imidazole), 2.33 (d, $J = 12.4$ Hz, 4H, $\text{C}(\text{CH}_3)_2\text{CH}_2$), 1.82 (s, 18H, $\text{C}(\text{CH}_3)_3$), 1.69 (s, 6H, $\text{C}(\text{CH}_3)_2\text{CH}_2$), 1.64 (s, 3H, $\text{C}(\text{CH}_3)_2\text{CH}_2$), 1.36 (s, 3H, $\text{C}(\text{CH}_3)_2\text{CH}_2$). ^{31}P NMR (CD_2Cl_2): $\delta = -143.40$ (septet, $J = 709.6$ Hz). ^{19}F NMR (CD_2Cl_2): $\delta = -72.46$ and -74.97 ($J = 707.9$ Hz). ^{13}C NMR (CD_2Cl_2): $\delta = 184.84$ (s, CO), 168.33 (s, C-carbenes), 121.56 (s, CH-imidazole), 118.44 (s, CH-imidazole), 65.23 (s, C^tBu), 59.21 (s, $\text{C}(\text{CH}_3)_2\text{CH}_2$), 33.24 (s), 31.26 (s, $\text{C}(\text{CH}_3)_3$), 29.98 (s), 25.42 (s, $\text{C}(\text{CH}_3)_2\text{CH}_2$). IR (CH_2Cl_2): $\nu(\text{CO})$ 2082, 2034 cm^{-1} . Anal. Calcd for $\text{C}_{24}\text{H}_{38}\text{F}_6\text{N}_4\text{O}_2\text{PIr}$ (751.77): C, 38.34; H, 5.09; N, 7.45. Found: C, 38.51; H, 4.97; N, 7.35.

Computational Details. The Amsterdam Density Functional (ADF) program was used to obtain all the geometries we discussed.^{44,45} The electronic configuration of the molecular systems was described by a triple- ζ STO basis set for iridium (4f, 5s, 5p, 5d, 6s, 6p), augmented with single p and f functions.⁴³ Triple- ζ STO basis sets were also used for chlorine (3s, 3p), nitrogen and carbon (2s, 2p), augmented with single d and f functions, and hydrogen (1s) augmented with single d and p functions. All these basis sets correspond to ADF basis set TZ2P.⁴³ The inner shells on rhodium and iridium (including 4d), chlorine (including 2p), and nitrogen and carbon (1s) were treated within the frozen core approximation. Energies and geometries were evaluated using the local exchange-correlation potential by Vosko et al.,⁴⁶ augmented in a self-consistent manner with Becke's⁴⁷ exchange gradient correction and Perdew's^{48,49} correlation gradient correction. Relativistic effects were included self-consistently with the zero-order relativistic approximation (ZORA).^{50,51} Since relativistic effects were included, the basis sets used were the relativistic basis sets (ZORA basis sets in ADF).

(44) *ADF 2000, Users Manual*; Vrije Universiteit: Amsterdam, The Netherlands, 2000.

(45) te Velde, G.; Bickelhaupt, F. M.; Baerends, E. J.; Fonseca Guerra, C.; Van Gisbergen, S. J. A.; Snijders, J. G.; Ziegler, T. *J. Comput. Chem.* **2001**, *22*, 931–967.

(46) Vosko, S. H.; Wilk, L.; Nusair, M. *Can. J. Phys.* **1980**, *58*, 1200–1211.

(47) Becke, A. *Phys. Rev. A* **1988**, *38*, 3098–3100.

(48) Perdew, J. P. *Phys. Rev. B* **1986**, *33*, 8822–8824.

(49) Perdew, J. P. *Phys. Rev. B* **1986**, *34*, 7406–7408.

(50) van Lenthe, E.; Baerends, E. J.; Snijders, J. G. *J. Chem. Phys.* **1993**, *99*, 4597–4610.

Molecular orbitals were plotted with the Molekel package.⁵² Natural bond order analysis⁵³ was performed with the Gaussian 03 program.⁵⁴ The ADF-optimized geometries were used for single-point calculations with the BP86 functional as implemented in the Gaussian 03 package. The SDD/ECP triple- ζ basis set was used for rhodium and iridium,⁵⁵ while the SVP double- ζ basis set with a polarization function was used for main group atoms.⁵⁶

Acknowledgment. The National Science Foundation is gratefully acknowledged for financial support of this work. L.C. thanks the University of Salerno for financial support (Grant Piccole Attrezzature di Ateneo 2002).

Supporting Information Available: Crystallographic information files (CIFs) of the complexes. This material is available free of charge via the Internet at <http://pubs.acs.org>. CCDC-254678–254684 (compounds **3**, **5**, and **7–11**) contain the supplementary crystallographic data for this paper. These data can be downloaded free of charge via www.ccdc.cam.ac.uk/conts/retrieving.html (or obtained from the Cambridge Crystallographic Data Centre, 12 Union Rd., Cambridge CB21EZ, U.K., fax (+44) 1223-336-033, e-mail deposit@ccdc.cam.ac.uk).

JA043249F

(51) van Lenthe, E.; Ehlers, A. E.; Baerends, E. J. *J. Chem. Phys.* **1999**, *110*, 8943–8953.

(52) MOLEKEL 4.0: P. Flükiger, H. P. Lüthi, S. Portmann, J. Weber, Swiss Center for Scientific Computing, Manno, Switzerland, 2000.

(53) Reed, A. E.; Curtiss, L. A.; Weinhold, F. *Chem. Rev.* **1988**, *88*, 899–926.

(54) Frisch, M. J.; Trucks, G. W.; Schlegel, H. B.; Scuseria, G. E.; Robb, M. A.; Cheeseman, J. R.; Montgomery, J. A.; Vreven, T.; Kudin, K. N.; Burant, J. C.; Millam, J. M.; Iyengar, S. S.; Tomasi, J.; Barone, V.; Mennucci, B.; Cossi, M.; Scalmani, G.; Rega, N.; Petersson, G. A.; Nakatsuji, H.; Hada, M.; Ehara, M.; Toyota, K.; Fukuda, R.; Hasegawa, J.; Ishida, M.; Nakajima, T.; Honda, Y.; Kitao, O.; Nakai, H.; Klene, M.; Li, X.; Knox, J. E.; Hratchian, H. P.; Cross, J. B.; Adamo, C.; Jaramillo, J.; Gomperts, R.; Stratmann, R. E.; Yazyev, O.; Austin, A. J.; Cammi, R.; Pomelli, C.; Ochterski, J. W.; Ayala, P. Y.; Morokuma, K.; Voth, G. A.; Salvador, P.; Dannenberg, J. J.; Zakrzewski, V. G.; Dapprich, S.; Daniels, A. D.; Strain, M. C.; Farkas, O.; Malick, D. K.; Rabuck, A. D.; Raghavachari, K.; Foresman, J. B.; Ortiz, J. V.; Cui, Q.; Baboul, A. G.; Clifford, S.; Cioslowski, J.; Stefanov, B. B.; Liu, G.; Liashenko, A.; Piskorz, P.; Komaromi, I.; Martin, R. L.; Fox, D. J.; Keith, T.; Al-Laham, M. A.; Peng, C. Y.; Nanayakkara, A.; Challacombe, M.; Gill, P. M. W.; Johnson, B.; Chen, W.; Wong, M. W.; Gonzalez, C.; Pople, J. A. *Gaussian 03*; Gaussian, Inc.: Pittsburgh, PA, 2003.

(55) Andrae, D.; Haeussermann, U.; Dolg, M.; Stoll, H.; Preuss, H. *Theor. Chim. Acta* **1990**, *77*, 123–141.

(56) Schäfer, A.; Horn, H.; Ahlrichs, R. *J. Chem. Phys.* **1992**, *97*, 2571–2577.